

# EXPERIMENTAL STUDY OF THE K-REGIME OF BREAKDOWN IN STRAIGHT AND SWEEP WING BOUNDARY LAYERS

V.G. Chernoray <sup>a)</sup>, A.A. Bakchinov <sup>b)</sup>, V.V. Kozlov <sup>a)</sup> and L. Löfdahl <sup>b)</sup>

<sup>a</sup> *Institute of Theoretical and Applied Mechanics, Novosibirsk, Russia*

<sup>b</sup> *Chalmers University of Technology, Thermo & Fluid Dynamics, Gothenburg, Sweden*

## I. INTRODUCTION

It is a well-known fact that the surface friction is the main source of drag on aircraft wings, road vehicles and other streamlined bodies. Since the skin friction of turbulent boundary layers is significantly greater than that of laminar boundary flows, it is most important to have an insight into how the laminar-turbulent transition occurs in different three-dimensional (3D) boundary layers. This knowledge would enable prediction and, in a future perspective, also control of all stages of the transition. However, it should be freely admitted that the understanding and the control of laminar-turbulent transition in such boundary layer flows have so far remained an unsolved problem of fluid dynamics. It has seen a slow development because of a great difficulty in solving this problem both numerically experimentally.

Whereas the stability of two-dimensional (2D) boundary layers has extensively been studied theoretically, experimentally and numerically, much less efforts have been devoted to the stability of 3D boundary layer flows due to complexity of phenomena underling the breakdown of laminar flow to turbulent stage [1]. Experiments on swept wing flows have revealed that different transition mechanisms can dominate in a given flow. The main instabilities are viscous, so-called Tollmien-Schlichting (T-S) instability, Görtler instability, cross-flow instability, and attachment-line instability. Although the cross-flow instability is considered to be the most “dangerous” one, our current work is directed toward studies of the transition caused by the unstable T-S waves, which can be observed in various 3D flows (e.g., boundary layers over straight and swept wings).

For 2D wall bounded shear flows two major types of transition are considered. At low level of external perturbations the ‘classic’, T-S transition scenario, is observed, whereas so-called ‘bypass’ transition scenario is associated with rather high level of environmental disturbances. The linear stability theory deals with the prediction whether a given flow is stable or not, and the theory can predict onset of transition and describe the initial linear stage. As far as non-linear waves evolution is concerned, two main regimes of transition have been identified and investigated experimentally. The K-regime, after Klebanoff et al. [2], and the N-regime, experimentally studied for the first time by Novosibirsk group, Kachanov et al. [3]). In the experimental work [4] it has been shown that both the initial spectral composition of interacting T-S waves and their initial amplitudes pre designate which of these regimes (competing with each other) occurs after the linear stage.

After the pioneer detailed experimental investigation of the K-breakdown scenario by Klebanoff et al. [2], several experimental works and theoretical studies have been conducted to adequately describe this phenomenon (e.g., see Hama and Nutant [5], Kachanov et al. [6], Herbert [7], Rist and Fasel [8]). The N-regime of transition was studied experimentally in detail a few years later (e.g., see Kachanov et al. [3], Saric, Kozlov and Levchenko [4], Kozlov et al. [9], Bake et al. [10], Fasel [11]). Comparisons between these two types of transition were discussed in Saric, Kozlov and Levchenko [4], Bake et al. [10], Laurén and Kleiser [12]. However, there is still a lack of experiments

and computations covering the non-linear evolution of disturbances in 3D boundary layer flows on airfoils at different sweep angles. In order to fill this gap, the generation and evolution of the viscous eigen-waves in 3D swept wing boundary layers have been experimentally studied and some of the results are presented in this paper.

## II. EXPERIMENTAL SET-UP

The experiment was conducted in a closed-circuit wind-tunnel with a test section of 1.8 m wide, 1.2 m height and 3 m length at the department of Thermo and Fluid Dynamics, Chalmers University of Technology, Göteborg, Sweden. A major series of experiments were conducted at the free-stream velocity  $U_o$  equal to 12.8 m/s. The free stream turbulence level in the test section was below  $0.001 U_o$  in the velocity range  $U_o = 5\text{--}15$  m/s (RMS was calculated in a frequency range 0.1–10000 Hz). All experiments were performed with a C-16 wing profile (500 mm chord, 1500 mm long and 80 mm thick, see *figure 1*), and the airfoil was mounted horizontally in the middle of the wind tunnel test section. An adjustable supporting mechanism was designed to adjust both the angle of attack and sweep. An existing traverse system was improved in order to study flow in transversal direction,  $Z$  (the experimental set-up and the coordinate system used are shown in *figure 1*). The traverse mechanism could position a hot-wire probe with precision of 1 mm in both  $Y$  and  $Z$  directions, and 5 mm in  $X$  direction. Preliminary tests were conducted with the airfoil at several sweep angles (0, 30 and 45 degrees), but the main series of experiments were performed at two sweep angles, namely, at zero sweep angle (a straight wing configuration) and 30 degrees (a swept wing configuration). The attack angle of the wing was chosen to obtain a weak adverse streamwise pressure gradient distribution in the measurement region over the working side of the airfoil (see *figure 2*). In this and subsequent figures the streamwise coordinate  $X$  is scaled with the wing cord,  $c$ , equal to 500 mm for the straight wing configuration, and 580 mm for the swept wing configuration. At this angle of attack no local separation of the flow was observed on the airfoil.

It was found that the transition to turbulence for both configurations was provoked by a rather high level sound field at frequency  $F_o = 300$  Hz. To obtain spatial-temporal flow patterns of the disturbed boundary layer the data acquisition was triggered with a signal from a microphone located in the test section.

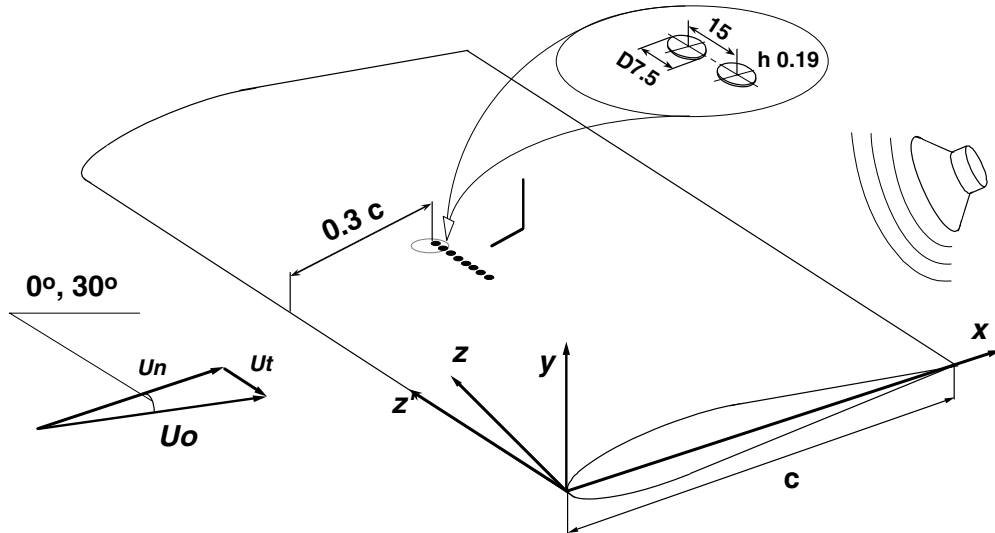


Figure 1. Scheme of the experimental set-up and actual coordinate system.

Roughness elements equidistantly aligned along the airfoil leading edge were placed on the surface to control a spanwise variation of the disturbance flow field in the boundary layers. The roughness elements stabilized the peak-and-valley Z-distribution of the wave amplitude and allowed us to study 3D dimensional patterns of the transitional boundary layer flow. The roughness array consisted of 10 cylindrical humps (7.5 mm diameter and 0.19 mm height) with spacing of  $\Delta Z_o = 15$  mm (see *figure 1* for detail). The roughness array was positioned at the chord region  $X/c = 0.30$  where the streamwise pressure gradient changed its sign from negative to positive. Previous experiments has clearly shown that in this region acoustic disturbances transform into eigen oscillation of the boundary layer (i.e. the highest receptivity of the boundary layer to acoustic waves was observed). The local Reynolds number based on the displacement thickness  $Re_{\delta^*}$  at the position of humps was about 600 and 640 for straight and swept wing configuration respectively, which corresponded to the boundary layer thickness  $\delta$  of 1.94 mm and 2.33 mm. Detailed mapping of the flow was made by a single, constant temperature hot-wire. The spanwise mean velocity component (crossflow) was measured with a custom V-shape two-wire boundary layer probe. The distance between centres of the wires was 1.2 mm.

As it was mentioned above, signals from hot-wire anemometers have been triggered with external sound measured with the microphone. The signals were then ensemble averaged (over 300 realizations) and stored in a PC for a subsequent analysis.

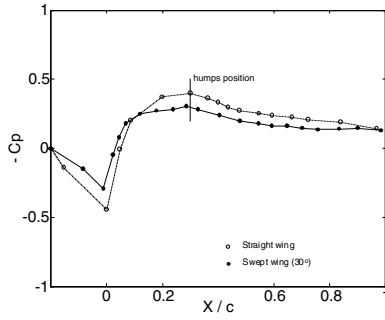


Figure 2. Chordwise pressure coefficients distribution for straight and swept wing configurations.

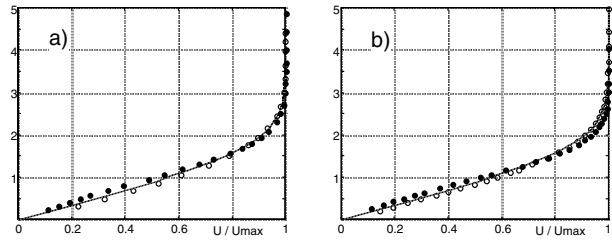


Figure 3. Mean streamwise velocity profiles on straight (a) and swept (b) wings compared with Blasius.  $X/c = 0.32$  — open circle symbols,  $X/c = 0.48$  — filled circle symbols.

As it can be seen from *figure 2* the weak adverse pressure gradient was established on the wing surface from  $X/c = 0.3$  for both configurations. Magnitude of the pressure gradient parameter  $dCp / d(X/c)$  was less than 0.9 in both cases. In the range of  $X/c = 0.5-0.7$  the pressure monotonically grows at about equal rates. The distribution of  $Cp$  does not reveal any local separation behaviour of the flow (there is no constant pressure plateau). *Figure 3* shows profiles of mean streamwise velocity measured at  $X/c = 0.32$  and  $0.48$  (corresponding Blasius profiles are shown with dotted lines). At first streamwise position the profiles are full, but further downstream they demonstrate decrease of the velocity near the wall for both straight and swept wing configuration.

Transformation of the sound at frequency 300Hz into boundary layer waves was observed at  $X/c = 0.3$  for both sweep angles. Waves grew as  $X$  increased, and resulted in the fully turbulent boundary layer flow at the last positions measured,  $X/c = 0.9$ . Amplitude-frequency spectra of some characteristic time traces are shown in *figure 4*. The non-linear evolution of the waves undergoes the stage of generation of super harmonics (600, 900Hz etc.). Further downstream resonant and combinational interactions between waves and random background disturbances eventually lead to complete randomization of the flow and typical turbulent spectra shown at  $X/c = 0.9$ . The first observation is that the non-linear evolution looks pretty the same for both straight and swept wing

configurations. Second note is that the transition on the straight airfoil seems to occur somewhat earlier than that on the swept wing due to different flow parameters (Reynolds number, pressure distribution). The time traces have been measured in boundary layer at constant distance  $Y$  from the airfoil surface at  $Z = 0$  (the centre of a roughness element).

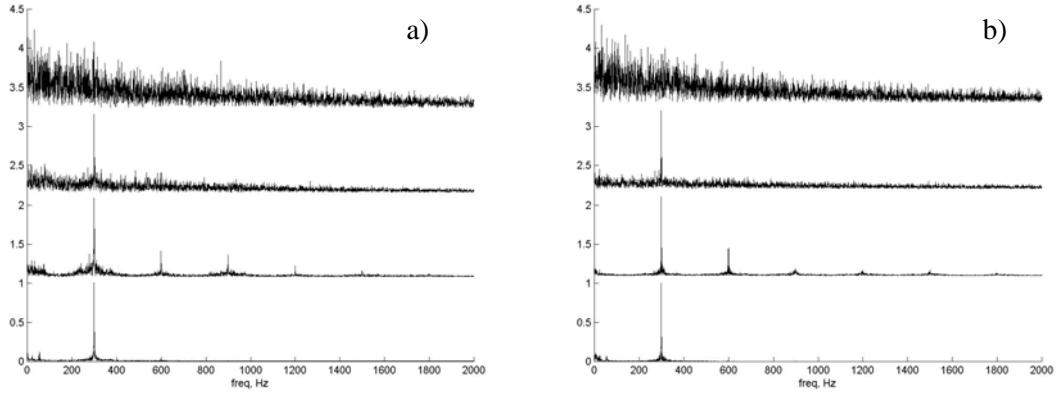


Figure 4. Amplitude-frequency spectra of time traces measured in straight (a) and swept (b) wing flows for different positions from noise  $X/c = 0.6, 0.7, 0.8, 0.9$ .  $Y = \text{const}$ . All spectra are undimensionalised by their maximum value.

Measurement in the span direction revealed that in the boundary layer spanwise modulated waves were observed for both configurations. Maxima in the spanwise wave amplitude distributions were found at position of spacers ( $Z\lambda_o = 1, 2 \dots$ , where  $\lambda_o = 1/Z_o$ ). At the downstream position  $X/c = 0.48$  the amplitude of the waves was measured and equal to  $0.39\% U_\infty$  and  $0.27\% U_\infty$  for the straight and the swept wing respectively, where  $U_\infty$  — a local streamwise velocity of inviscid flow. Phase velocity of the waves  $c_r$  was found to be of  $0.41U_o$  ( $\lambda_r = 17.5 \text{ mm}$ ) with the wave front parallel to the leading edge. In the case of the straight wing configuration the spanwise modulation of wave is symmetrical and corresponds to combination of the plane spectral mode  $(F_o, 0)$  and two oblique modes  $(F_o, \pm \lambda_o)$  in Fourier space. For the swept wing the modulation does not seem to be symmetrical and corresponding frequency-spanwise wavenumber spectra consist of the mode  $(F_o, 0)$  and only one oblique mode  $(F_o, \lambda_o)$ . Non-linear interacting waves grow downstream with formation of ‘peak’ and ‘valley’ structures in span direction. High amplitudes of perturbations were found in peak positions. On *figure 4*, left, at  $X/c = 0.66$  nonlinear stage of disturbance development is shown. Amplitude of disturbances is more than  $15\%$  of  $U_\infty$  for both configurations.

In the straight wing boundary layer so-called  $\Lambda$ -structures were mapped similar those observed by Klebanoff et al. [2], whereas in the swept wing boundary layer non-symmetrical structures were obtained.

It should be noted that non-symmetry of the basic (mean) boundary layer flow (for the swept wing) results in non-symmetry of the disturbance flow patterns at non-linear stage of evolution of the waves (see *figure 5*). Fourier decompositions show growth of modes  $(F_o, \pm 2\lambda_o)$  in the case of straight wing (formation of ‘legs’ of the  $\Lambda$ -structures). Evolution of the spectra for the swept wing configuration differs from that for the straight wing. At the initial stages of the non-linear evolution damping of  $(F_o, \lambda_o)$ -mode takes place, accompanying with the amplification of anti-symmetrical  $(F_o, -\lambda_o)$ -mode. Further downstream, the growth of  $(F_o, -2\lambda_o)$ -mode occurs accompanying with decaying  $(F_o, 0)$ -mode. Flow structures shown on (*figure 5, d*) are mostly

associated with modes  $(F_o, 0)$ ,  $(F_o, -\lambda_o)$  and  $(F_o, -2\lambda_o)$ . As we pointed out above, the main reason of the non-symmetry of the flow patterns is the presence of the crossflow.

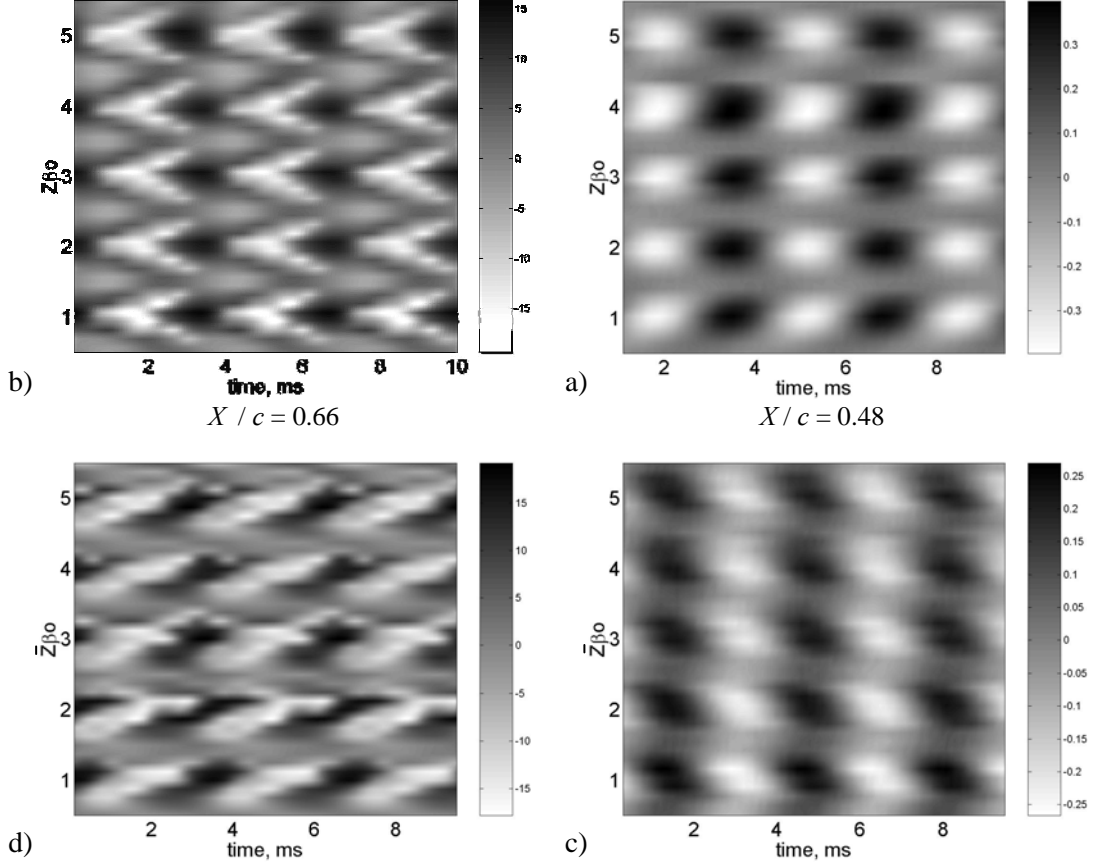


Figure 5. Patterns of the ensemble averaged streamwise velocity disturbance component in  $(t, z)$ -planes revealing the scenario of transition in straight (a, b) and swept (c, d) wing flows.  $X/c = 0.48$  (a, c),  $X/c = 0.66$  (b, d).

In the experiments by Grek et al. [13] it was shown that crossflow could cause the formation of non-symmetry in streaky-structures. In their experiments a solitary streaky-structure was generated in the boundary layer by means of injection of a portion of air through transversal slot on the swept wing surface. To check those results the detailed measurements of crossflow have been done (figure 6). In the boundary layer of the swept wing our measurements have shown that the non-zero crossflow velocity component can be observed in all streamwise positions measured. At the position of roughness elements,  $X/c = 0.3$ , magnitude of the  $W$  velocity was found to be up to 10 % of  $U_o$  inside boundary layer, and about 6% of  $U_o$  at the outer edge of boundary layer. Further downstream the crossflow component is almost constant from  $X/c = 0.5$  to  $X/c = 0.8$  with magnitude of 3% of  $U_o$ .

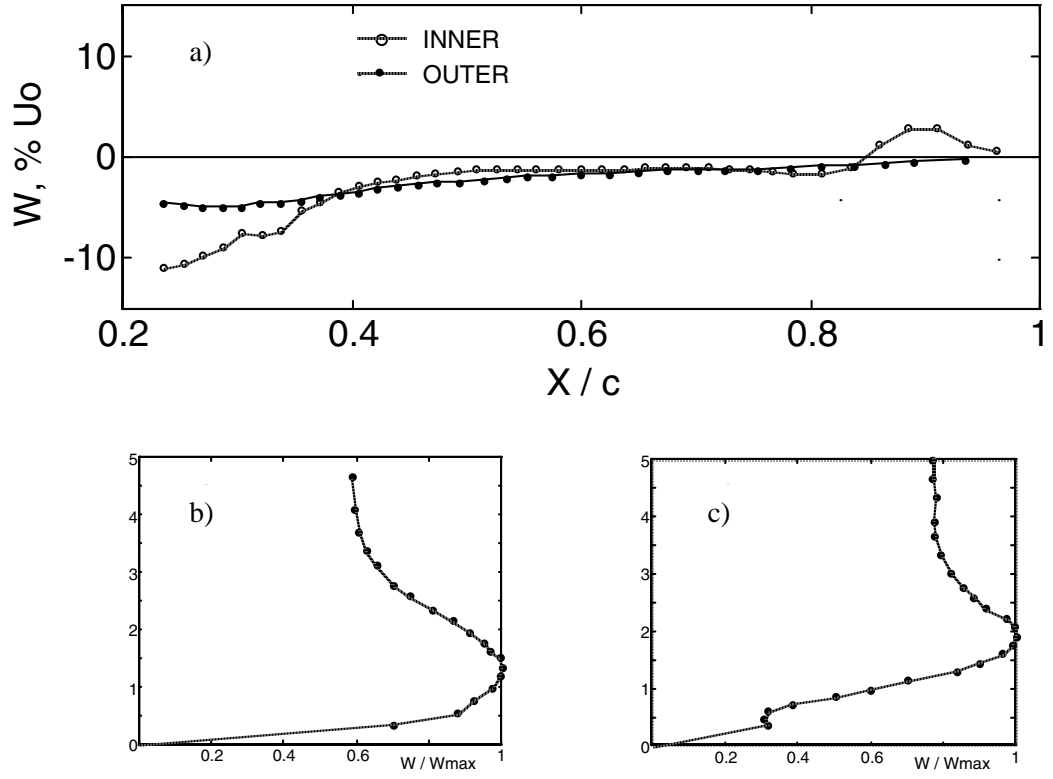


Figure 6. Results of crossflow measurements on swept wing. Chordwise mean crossflow distribution (a) for inviscid flow (OUTER) and inside boundary layer (INNER) for  $Y$  position.. Distribution of mean crossflow velocity across boundary layer:  $X/c = 0.32$  (b) and  $X/c = 0.48$  (c).

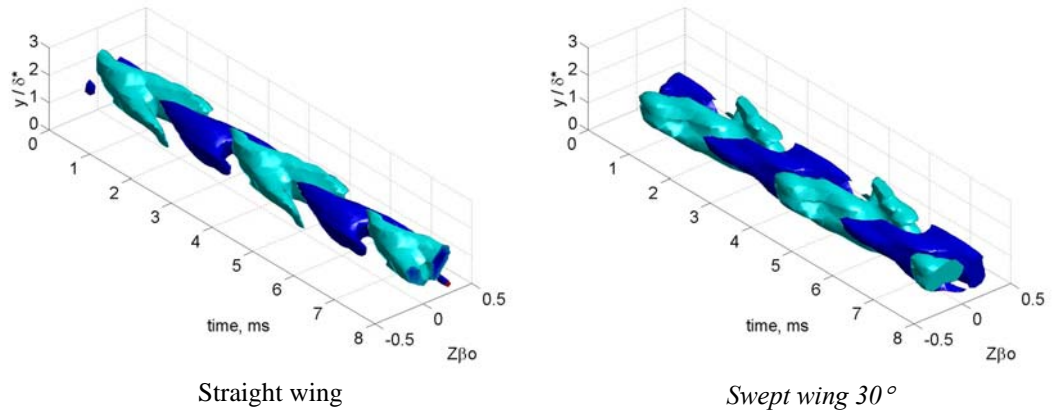


Figure 7. Isosurfaces of the ensemble averaged streamwise velocity disturbance component  $u = 8\% U_\infty$  — dark shading,  $u = -8\% U_\infty$  — light shading.  $X/c = 0.66$ .  $\Lambda$ -structures in straight wing flow (a), non-symmetrical structures in swept wing flow (b).

The step on the INNER curve at  $X / c = 0.3$  (see *figure 6*) is due to streamlines displacement caused by the roughness elements. After  $X / c = 0.85$  the crossflow component of velocity change its sign from negative to positive. *Figure 5* shows  $\Lambda$ -structures in  $(Y, Z, t)$  coordinates for straight wing and non-symmetrical structures for the swept wing flow. It is evident that structures in both cases are different not only at one given  $Y$ -position, but across the boundary layer. High-shear layer is formed near the ‘head’ and ‘shoulders’ of the lambda-structures in the straight wing flow, as it was observed in experiments on flat plate boundary layer [2, 3, 6, 10]. In swept wing flow there are two regions of high-shear layer along each structure. It can be concluded that, due to the crossflow, the temporal-spatial structures of the disturbed flow field over swept wing have revealed significant differences in K-type transition to turbulence.

## Conclusion

The experiments on stability of three-dimensional boundary layer on the straight and swept airfoils were conducted. A detailed measurements of the streamwise velocity field in  $(Y, Z)$  plane have revealed both linear and non-linear evolutions of disturbances generated in the airfoil boundary layers by external acoustic field. To the best of our knowledge this is the first experimental work where the K-regime of transition on a swept wing model has been observed and compared with that on the straight wing model at other conditions been equal.

## References

1. Reed H.L. & Saric W.S., 1989, Stability of three-dimensional boundary layers, *Annu. Rev. Fluid. Mech.*, Vol. 21, pp. 235–284.
2. Klebanoff P.S., Tidstrom K.D. and Sargent L. M., 1962, The three-dimensional nature of boundary layer instability, *J. Fluid Mech.*, Vol. 12, pp. 1–34.
3. Kachanov Y.S., Kozlov V.V., Levchenko V.Y., 1977, Nonlinear development of a wave in a boundary layer, *Izv. Akad. Nauk SSSR, Mekh. Zhidk. Gaza*, Vol. 5, pp. 85-94 (in Russian). Transl. *Fluid. Dyn.*, Vol. 12 (1978), pp. 383–390.
4. Saric W., Kozlov V., Levchenko V., 1984 Forced and unforced subharmonic resonance in boundary layer transition, *AIAA Paper No. 84-0007*.
5. Hama F., Nutant J., 1963, Detailed flow-field observations in the transition process in a thick boundary layer, in: *Proc. Heat Transfer and Fluid Mech. Inst.*, Stanford Univ. Press, CA, pp. 77–93.
6. Kachanov Y.S., Kozlov V.V., Levchenko V.Y., Ramazanov M., 1984 Experimental study of the K-regime breakdown of a laminar boundary layer, *Preprint No. 9-84. Inst. Theoret. Appl. Mech., USSR Acad. Sci.*, Novosibirsk (in Russian).
7. Herbert T., 1988, Secondary instability of boundary layers, *Annu. Rev. Fluid Mech.*, Vol. 20, pp. 487–526.
8. Rist U., Fasel H., 1995, Direct numerical simulation of controlled transition in a flat-plate boundary layer, *J. Fluid Mech.*, Vol. 298, pp. 211–248.
9. Kozlov V.V., Levchenko V.Y. & Saric W. S., 1983, Formation of three-dimensional structures in a boundary layer at transition, *Preprint No. 10-83. Inst. Theoret. Appl. Mech., USSR Acad. Sci.*, Novosibirsk (in Russian).
10. Bake S., Fernholz H.H., Kachanov Y.S., 2000, Resemblance of K- and N-regimes of boundary layer transition at late stages, *Eur. J. Mech. B – Fluids*, Vol 19, pp. 1–22.
11. Fasel H., 1990, Numerical simulation of instability and transition in boundary layer flows, in: *Arnal D., Michel R. (Eds), Laminar Turbulent Transition*, Springer, Heidelberg, pp. 587–598.
12. Laurien E., Kleiser L., 1989, Numerical simulation of boundary layer transition and transition control, *J. Fluid Mech.*, Vol. 199, pp. 403–440.
13. Grek G.R., Katasonov M.M., Kozlov V.V., Chernoray V.G., 1999, Modelling of streaky-structures in two- and three-dimensional boundary layers, *Preprint No. 2-99. Inst. Theoret. Appl. Mech., Russian Acad. Sci.*, Novosibirsk (in Russian).